



## Relative quantitation goes viral: An RT-qPCR assay for a grapevine virus



R. Bester<sup>a</sup>, P.T. Pepler<sup>a</sup>, J.T. Burger<sup>a</sup>, H.J. Maree<sup>a,b,\*</sup>

<sup>a</sup> Department of Genetics, Stellenbosch University, Private Bag X1, Matieland 7602, South Africa

<sup>b</sup> ARC Infruitec-Nietvoorbij (The Fruit, Vine and Wine Institute of the Agricultural Research Council), Private Bag X5026, Stellenbosch 7599, South Africa

### ABSTRACT

#### Article history:

Received 2 July 2014

Received in revised form

16 September 2014

Accepted 24 September 2014

Available online 5 October 2014

#### Keywords:

GLRaV-3

Relative quantification

RT-qPCR, Subgenomic RNA

Grapevine leafroll disease

SYBR green

Accurate detection and quantitation of viruses can be beneficial to plant–virus interaction studies. In this study, three SYBR green real-time RT-PCR assays were developed to quantitate *grapevine leafroll-associated virus 3* (GLRaV-3) in infected vines. Three genomic regions (ORF1a, coat protein and 3'UTR) were targeted to quantitate GLRaV-3 relative to three stably expressed reference genes (actin, GAPDH and  $\alpha$ -tubulin). These assays were able to detect all known variant groups of GLRaV-3, including the divergent group VI, with equal efficiency. No link could be established between the concentration ratios of the different genomic regions and subgenomic RNA (sgRNA) expression. However, a significant lower virus concentration ratio for plants infected with variant group VI compared to variant group II was observed for the ORF1a, coat protein and the 3'UTR. Significant higher accumulation of the virus in the growth tip was also detected for both variant groups. The quantitation of viral genomic regions under different conditions can contribute to elucidating disease aetiology and enhance knowledge about virus ecology.

© 2014 Elsevier B.V. All rights reserved.

### 1. Introduction

A complex network of cellular processes regulates gene expression in plants to ensure normal development and appropriate responses to environmental stresses. Biotic stresses from fungal, bacterial and viral pathogens are a major constraint to the production of agricultural crops. It is therefore imperative to understand plant–pathogen interactions before translating this knowledge into management strategies. Research into plant–pathogen interactions can be approached from the perspective of the host plant or the pathogen (Boyd et al., 2013). Studying the host will lead to the identification of genes involved in partial or permanent pathogen resistance while studying the pathogen leads to the identification of factors that could trigger the plant's defence response. Both approaches benefit from accurate detection and quantitation of the pathogen. Specifically for viruses, the quantitation of not only the viral particles with ELISA, but also different viral genes with RT-qPCR can contribute to our understanding of the disease aetiology.

Reverse transcription quantitative PCR (RT-qPCR) is currently one of the most sensitive techniques for analysing gene

expression and has been applied for viral quantitation (Eun et al., 2000; Roberts et al., 2000). RT-qPCR assays can utilise fluorescent dyes or probe-based chemistry (Bustin, 2000) and quantitation will involve either an absolute or relative quantitation strategy (Pfaffl, 2001). For viruses, the detection and quantitation can be complicated by low virus concentration and the presence of diverse variants. Therefore, a sensitive RT-qPCR assay that can detect all virus variants with equal efficiency can aid research focussed at plant–virus interactions.

Grapevine is a highly valuable agricultural commodity that is host to the largest number of viruses of any crop plant (Martelli and Boudon-Padieu, 2006; Prosser et al., 2007). For the purpose of this study we focused on *Grapevine leafroll-associated virus 3* (GLRaV-3), believed to be the main aetiological agent of Grapevine leafroll disease (GLD) (Maree et al., 2013). GLRaV-3 is the type species of the genus *Ampelovirus* in the family *Closteroviridae* (Martelli et al., 2012). Currently, the complete genomes of only ten distinct GLRaV-3 isolates are available that can be divided into four major genetic variant groups (Engel et al., 2008; Maree et al., 2008; Jarugula et al., 2010; Jooste et al., 2010; Gouveia et al., 2011; Sharma et al., 2011; Wang et al., 2011; Bester et al., 2012a; Seah et al., 2012; Fei et al., 2013). The isolates of GLRaV-3 are 91% similar when variant group I is compared to variant group II and 88% when variant group I is compared to variant group III. However, isolates from variant group VI are less than 70% identical to isolates from variant groups I–III

\* Corresponding author at: Department of Genetics, Stellenbosch University, Private Bag X1, Matieland 7602, South Africa. Tel.: +27 21 808 9579.

E-mail addresses: [hjmaree@sun.ac.za](mailto:hjmaree@sun.ac.za), [mareeh@arc.agric.za](mailto:mareeh@arc.agric.za) (H.J. Maree).

(Bester et al., 2012a). Three additional variant groups have also been identified, but are only represented by partial sequences (Gouveia et al., 2011; Sharma et al., 2011; Chooi et al., 2013a). Recently, two new GLRaV-3 isolates, GH24 (GenBank: KM058745) and GTG10 (Goszczynski, 2013), were identified. They were found to be more diverse compared to known variant groups and have not yet been assigned to a group. This finding further highlights the great extent of genetic variability between variant groups of GLRaV-3 and warrants the search for a universal detection system.

Currently, the industry standard for GLRaV-3 detection is enzyme-linked immunosorbent assays (ELISA) and conventional end-point RT-PCRs. ELISAs can be time consuming and lack the sensitivity needed for the detection of low virus concentration. Standardised ELISA protocols for GLRaV-3 are also not able to detect all GLRaV-3 variants with equal sensitivity (Cohen et al., 2012). Improvement in the specificity and sensitivity of detection has been achieved by the introduction of qPCR assays based on fluorescent detection systems. Both SYBR green and hydrolysis probe qPCR have been used for the diagnosis and/or quantitation of several grapevine viruses, including GLRaV-3 (Osman and Rowhani, 2006; Osman et al., 2007, 2008; Margaria et al., 2009; Pacifico et al., 2011; Bester et al., 2012b; Tsai et al., 2012; Chooi et al., 2013b; López-Fabuel et al., 2013).

In this study three sensitive SYBR green RT-qPCR assays were developed that are able to detect all variant groups (groups I–III, VI and GH24-like) of GLRaV-3 known to be present in South Africa with equal efficiency. These assays enabled the evaluation of different virus genome regions for their suitability for accurate calculation of GLRaV-3 virus concentration in infected phloem material. The RT-qPCR assays described in this study provide tools for the study of virus ecology.

## 2. Materials and methods

### 2.1. Plant material and sample preparation

Six *Vitis vinifera* cultivar Cabernet Sauvignon plants, from a virus isolate collection (Vitis Laboratory, Stellenbosch University, South Africa), were pruned back and left to grow for 60 days in the greenhouse. Only one shoot was allowed to grow and all side shoots were constantly removed. Three plants each, infected with GLRaV-3 variant group II and VI, respectively were selected. Plants were negative for frequently occurring grapevine viruses, except GLRaV-3. GLRaV-3 variant group status of all plants was confirmed using the previously designed real-time RT-PCR high-resolution melting curve analysis assay (Bester et al., 2012b). The shoot from each plant was divided into 5 equal segments to represent different growth stages with segment 1 representing the older (bottom) part of the shoot and segment 5 the actively growing young material at the top of the plant. Due to GLRaV-3 being a phloem-limited virus, phloem material of each segment was collected and stored at  $-80^{\circ}\text{C}$ .

### 2.2. Total RNA extraction

Total RNA was extracted from 2 g of phloem material using a modified CTAB extraction protocol (Carra et al., 2007). The CTAB buffer contained 2% CTAB, 2.5% PVP-40, 100 mM Tris-HCl (pH8), 2 M NaCl, 25 mM EDTA (pH8) and 2%  $\beta$ -mercaptoethanol. Total RNA was precipitated by adding 2.5 volumes 100% ethanol and 0.1 volumes 3 M sodium acetate (pH5.2) to the upper phase of the 5 M NaCl and chloroform-isoamyl alcohol (24:1) extraction step (Carra et al., 2007). RNA was precipitated for 1 h at  $-20^{\circ}\text{C}$  and centrifuged at 13,500 rpm for 30 min at  $4^{\circ}\text{C}$ . Pellets were washed with 80% ethanol and resuspended in 100  $\mu\text{l}$  Milli-Q H<sub>2</sub>O (Millipore Corporation, Billerica, USA). Integrity and purity was assessed using agarose gel

electrophoresis and spectrophotometry (NanoDrop ND-100, NanoDrop Products, Wilmington, USA).

10  $\mu\text{g}$  of total RNA was treated with RQ1 RNase-free DNase (Promega, Madison, USA) in 50  $\mu\text{l}$  reactions according to manufacturer's instructions. 450  $\mu\text{l}$  of 10 mM Tris-HCl (pH 8.5) was added to the DNase treatment mixture and an acidic phenol: chloroform-isoamyl alcohol (5:1) extraction was performed with an ethanol and sodium acetate precipitation (2.5 volumes of 100% ethanol and 0.1 volumes of 3 M Sodium acetate (pH5.2)). After a wash step with 80% ethanol, pellets were dried and resuspended in 30  $\mu\text{l}$  Milli-Q H<sub>2</sub>O. Integrity and purity was assessed using agarose gel electrophoresis and spectrophotometry.

### 2.3. cDNA synthesis

Complementary DNA (cDNA) were synthesised from 1  $\mu\text{g}$  of total RNA using 0.15  $\mu\text{g}$  random hexamers (Promega) and Avian myeloblastosis virus (AMV) reverse transcriptase (Thermo Scientific, Massachusetts, USA) in a final volume of 20  $\mu\text{l}$  according to manufacturer's instructions. 10  $\mu\text{l}$  of each cDNA sample was pooled and a 5-fold dilution series was prepared to construct standard curves for all primer sets. The remaining cDNA was diluted 1:24 and treated as the unknown samples for quantitation. All cDNA dilutions were stored at  $-20^{\circ}\text{C}$ .

### 2.4. Primer design

Primers were designed targeting three different regions of the GLRaV-3 genome. Open reading frame 1a (ORF1a), ORF6 (coat protein) and the 3'UTR were selected to represent genes/regions with different levels of subgenomic RNAs (sgRNAs) (Jarugula et al., 2010; Maree et al., 2010). By constructing a multiple sequence alignment using CLC main workbench 6.5 (CLC bio, Aarhus, Denmark), conserved regions in the chosen genes/regions of GLRaV-3 were identified. All the GLRaV-3 complete genomes available (GenBank: AF037268.2, GenBank: JQ423939.1, GenBank: JQ655296.1, GenBank: JQ655295.1, GenBank: EU259806.1, GenBank: EU344893.1, GenBank: JX559645.1, GenBank: JQ796828.1, GenBank: GQ352633.1, GenBank: GQ352632.1, GenBank: GQ352631.1, GenBank: GU983863.1, GenBank: KM058745) were included in the multiple sequence alignment in order to design primers that were able to detect all variant groups known to be present in South Africa. All primers were subjected to an NCBI BLAST screen for specificity. Five different primer sets targeting *Vitis vinifera* reference genes were selected from the Reid et al. (2006) study to evaluate their expression stability across all samples used in this study.

### 2.5. RT-qPCR

#### 2.5.1. PCR and cycle conditions

RT-qPCRs were performed using the Rotor-Gene Q thermal cycler (Qiagen, Venlo, Netherlands) and the SensiMix™ SYBR No-ROX Kit (Bioline, Taunton, USA). Reactions contained 2 $\times$  SensiMix™ SYBR No-ROX, Milli-Q H<sub>2</sub>O and 0.4, 0.48 or 0.56  $\mu\text{M}$  forward and reverse primers (IDT, Coralville, USA), depending on the primer set (Table 1). 2.5  $\mu\text{l}$  cDNA was added to each reaction to a final reaction volume of 12.5  $\mu\text{l}$ . The same cDNA dilution series was used to construct all eight primer-specific standard curves and the same 1:24 dilution of each of the "unknown" samples was screened with the eight primer sets for quantitation. No-template controls, negative plant controls (negative for GLRaV-3) and the third dilution point (1/25) of the five-fold dilution series were included in all runs. To test for the extent of genomic DNA contamination "no-reverse transcription" control qPCRs were performed for all samples using an intron-spanning primer set for the actin gene.

**Table 1**  
Primer sets targeting GLRaV-3 genomic regions of interest and *Vitis vinifera* reference genes.

Primer	Sequence	Amplicon size	Target	Primer concentration ( $\mu\text{M}$ )	Annealing temperature ( $^{\circ}\text{C}$ )	Reference
LR3.6995F	GGGRACGGARAAGTGTACC	144	GLRaV-3	0.4	53	This study
LR3.7138R	TCCAAYTGGGTCATRCACAA		ORF1a			
LR3.14586F	ATGAAYGARAARGTYATGGC	140	GLRaV-3 Coat protein (CP)	0.48	50	This study
LR3.14725R	CTAACACGYTGYTGYCTAG					
LR3.18345F	CCTCACGGTTAATACTCTG	144	GLRaV-3 3' untranslated region (3'UTR)	0.4	54	This study
LR3.18488R	ATTGTCGATAAGTTAGCCTC					
Vv.actin.F	CTTGCATCCCTCAGCACCTT	82	<i>Vitis vinifera</i> actin	0.4	55	Reid et al. (2006)
Vv.actin.R	TCCTGTGGACAATGGATGGA					
Vv. $\alpha$ -tubulin.F	CAGCCAGATCTTCACGAGCTT	119	<i>Vitis vinifera</i> alpha-tubulin	0.4	55	Reid et al. (2006)
Vv. $\alpha$ -tubulin.R	GTTCTCGCGCATTGACCATA					
Vv.UBC.F	GAGGGTCGTCAGGATTGGA	75	<i>Vitis vinifera</i> Ubiquitin-conjugating enzyme	0.4	55	Reid et al. (2006)
Vv.UBC.R	GCCCTGCACCTTACCATCTTAAAG					
Vv.GAPDH.F	TTCTCGTTGAGGGCTATTCCA	70	<i>Vitis vinifera</i> Glyceraldehyde 3-phosphate dehydrogenase	0.4	55	Reid et al. (2006)
Vv.GAPDH.R	CCACAGACTTCATCGGTGACA					
Vv.EF1 $\alpha$ .F	GAAGTGGGTGCTGATAGGC	150	<i>Vitis vinifera</i> Elongation factor 1-alpha	0.56	55	Terrier et al. (2005)
Vv.EF1 $\alpha$ .R	AACCAAAATATCCCGAGTAAAAGA					

All reactions were performed in triplicate in Qiagen Rotor-Gene Q 0.1 ml tube-and-cap strips. Cycling parameters included an initial activation of 95  $^{\circ}\text{C}$  for 10 min and 45 cycles of 95  $^{\circ}\text{C}$  for 15 s, primer-specific annealing temperature for 15 s (Table 1) and 72  $^{\circ}\text{C}$  for 15 s. Acquisition on the green channel was recorded at the end of the extension step. Melting curve analysis of PCR amplicons was performed with temperatures ranging from 65  $^{\circ}\text{C}$  to 95  $^{\circ}\text{C}$  with a 1  $^{\circ}\text{C}$  increase in temperature every 5 s to identify primer-dimers and non-specific amplification.

### 2.5.2. Single-variant efficiency

To be able to calculate accurately the relative quantity of viral genomes, irrespective of GLRaV-3 variant status, the PCR efficiency of different GLRaV-3 single-variant infections were compared. GLRaV-3 single-variant infected samples were collected from a virus isolate collection (Vitis Laboratory, Stellenbosch University, South Africa), processed and treated as described above. These samples represented Groups I–VI, as well as isolate GH24. A five-fold dilution series was prepared from the cDNA and standard curves constructed for each variant group separately. PCR efficiencies were calculated for all GLRaV-3 primer sets (Rasmussen, 2001, Eq. (1)).

### 2.5.3. Relative limit of detection

The sensitivity of each GLRaV-3 primer set was evaluated and compared by using the five-fold cDNA dilution series used to construct standard curves in this study. The same dilution series was used for all primer sets in both real-time PCR and conventional end-point PCR instruments. The real-time PCRs were performed according to the conditions described above. In the end-point PCRs, a 2.5  $\mu\text{l}$  aliquot of cDNA was added to a 25  $\mu\text{l}$  PCR reaction mixture containing 1  $\times$  KAPA Taq buffer A (KAPA Biosystems, Cape Town, South Africa), 0.4 mM dNTP mix (Thermo Scientific), 0.4–0.48  $\mu\text{M}$  forward and reverse primers (IDT) (Table 1) and 0.08 U/ $\mu\text{l}$  KAPA Taq DNA polymerase (KAPA Biosystems). Cycle conditions included an initial denaturation step at 94  $^{\circ}\text{C}$  for 5 min, followed by 35 cycles of 94  $^{\circ}\text{C}$  for 15 s, primer-specific annealing temperature for 15 s and elongation at 72  $^{\circ}\text{C}$  for 15 s. Final extension was at 72  $^{\circ}\text{C}$  for 7 min. Amplicons were visualised on an ethidium bromide-stained 2% TAE agarose gel (2 M Tris, 1 M glacial acetic acid, 0.05 M Na<sub>2</sub>EDTA, pH 8).

### 2.5.4. Reference gene stability test

In order to find reference gene mRNA that is stably expressed in phloem material across the length of a growing grapevine shoot, five *V. vinifera* reference genes were selected (Table 1). The quantitation cycle ( $C_q$ ) data (see Section 2.5.5 for  $C_q$  calculation) from all

30 samples (six plants, five samples each) were used to calculate stability of reference gene expression using two Excel-based applications, Normfinder (Andersen et al., 2004) and BestKeeper (Pfaffl et al., 2004).

### 2.5.5. Data analysis

The PCR efficiency ( $E$ ) for each of the targets was calculated using the slope of the standard curve constructed with the five-fold dilution series over the linear dynamic range consistent between the primer sets (2nd (1/5) to 6th (1/3125) dilution point) (Eq. (1)). The relative virus concentration ratio (VCR) was calculated by an efficiency correction mathematical model using reference gene normalisation (Pfaffl, 2001). The original (Pfaffl, 2001) model utilises only the slope and  $C_q$  variables due to the  $y$ -intercept ( $b$ ) being equal for the control and sample group (Eq. (2)). However, since no  $C_q$  value will be obtained for samples negative for GLRaV-3, the control group will be absent and the influence of  $b$  should be considered. The  $C_q$  values for all samples were calculated using the threshold cycle method (Pfaffl, 2004). After importing the primer-specific standard curve in each Rotor-Gene Q run,  $b$  was adjusted using the third dilution of the standard curve. This standard was included in each run, to compensate for inter-assay variation. The geometric mean of the triplicate reactions of each sample was used for all calculations. The three most stable reference genes (*ref*) were selected for normalisation and a reference gene index (RGI) was calculated using their geometric mean (Eq. (3)). Normalisation of the viral gene quantitation values, to calculate the relative VCR, was performed using the RGI and not a single reference gene (Eq. (4)) (Vandesompele et al., 2002). The Rotor-gene Q software version 2.2.3 (Qiagen) was used to calculate primer efficiencies,  $C_q$  values and gene quantitation values for all targets. The relative VCRs were calculated using Eq. (4):

$$E = 10^{[-1/\text{slope}]} \quad (1)$$

$$\text{Quantitation value (conc)} = 10^{\frac{(C_q - b)}{\text{slope}}} \quad (2)$$

$$\text{RGI} = \sqrt[3]{(\text{conc}_{\text{ref1}}) \times (\text{conc}_{\text{ref2}}) \times (\text{conc}_{\text{ref3}})} \quad (3)$$

$$\text{VCR}_{(\text{multiple reference genes})} = \frac{\text{conc}_{\text{target}}}{\text{RGI}} \quad (4)$$

### 2.5.6. Statistical models

A number of statistical models were fitted using SAS Enterprise Guide version 5.1 (SAS Institute, NC, USA). Due to the distribution of VCRs being positively skewed, the data were transformed using the natural logarithm (log base  $e$ ) to meet the distributional assumptions (normality and homoscedasticity) of the statistical

models applied. Different linear mixed effect models (Snijders and Bosker, 1999) were fitted in order to identify statistical differences in VCR between plants infected with different GLRaV-3 variants, measured using different GLRaV-3 genomic regions and different plant segments. The “plant  $\times$  assay” combinations were used as the subjects (replications), and the different plant segments were analysed as the within-subject effect. Unstructured covariance matrices were assumed for the linear mixed effects models fitted for the effects associated with each variant group’s *plant segments* and *genomic regions*. However, investigation into the differences between *variant groups* based on the three different *genomic regions* required constraints on the covariance matrices due to the small sample size. For these three linear mixed effects models, the variance components covariance matrix model was used. Analysis of variance (ANOVA) for repeated measurements was performed to determine statistical significance of the effects. Bonferroni-type adjustments (Altman, 1990) were made to the *p*-values to control the family-wise Type I error rate. All Bonferroni-adjusted *p*-values are indicated as “(Adj *p*-value = . . .)”. A significance level of 5% was used.

### 3. Results

#### 3.1. Plant material

After 60 days, the six plants had an average shoot length of 248.2 cm ( $\pm 38.9$  cm) and each plant was divided into five equal segments with an average length of 49.6 cm ( $\pm 7.8$  cm). The mature shoots were in the pre-lignification phase with mature leaves for segments one to four. Segment five had smaller leaves and tendrils. A gradual colour change from dark green to light green was observed for segment one to five. The leaves, tendrils, periderm and apical meristem were removed before phloem material was sampled from the shoots. For segment four and five, no differentiation was possible between the periderm and phloem layer. The GLRaV-3 variant status of each plant was confirmed. GH33, GH34 and GH36 were singly infected with variant group II and GH27, GH29 and GH30 were singly infected with GLRaV-3 variant group VI.

#### 3.2. RNA extraction

Total RNA extraction resulted in an average yield of 1028 ng/ $\mu$ l (100  $\mu$ l) with an average A260/A280 ratio of 1.97 and an average A260/A230 ratio of 2.21. After DNase treatment of 10  $\mu$ g of total RNA the average yield was 265 ng/ $\mu$ l (30  $\mu$ l) with an average A260/A280 ratio of 1.84 and an average A260/A230 ratio of 2.16. DNase treatment resulted in an averaged yield loss of 37%. No RNA degradation could be detected with gel electrophoresis, before or after DNase treatment.

#### 3.3. Primer specificity

Specificity of all primers was evaluated based on gel electrophoresis and melting curve analysis. Gel electrophoresis showed a single amplicon of the desired size for all primer sets (Table 1). The Rotor-Gene Q melting curve analyses resulted in a single amplicon-specific melting temperature for each reference gene and an amplicon-specific melting temperature for each variant group of GLRaV-3 (Supplementary Table 1). Sanger sequencing confirmed all single variant infections. Sequencing results also confirmed the specificity of the three GLRaV-3 primer sets. Primer dimers were detected in only the “No-template” control reactions of the CP ( $C_q > 35$ ) and actin primer sets ( $C_q > 36$ .) and in the negative plant control reactions of the ORF1a ( $C_q > 32$ ) and CP primer sets ( $C_q > 29$ ). No primer dimers were detected in any

**Table 2**

Efficiency, coefficients of determination ( $r^2$ ), slope and *y*-intercept (b) of standard curves constructed using the Rotor-Gene Q software.

Assay	Efficiency	$r^2$	Slope	<i>y</i> -intercept (b)
ORF1a	1.02	0.996	−3.286	20.623
CP	1.01	0.997	−3.287	19.707
3'UTR	1.01	0.994	−3.298	20.786
actin	0.99	0.997	−3.349	17.746
GAPDH	1.01	0.997	−3.305	20.615
$\alpha$ -Tubulin	1.00	0.996	−3.317	20.090
UBC	1.02	0.991	−3.273	22.042
EF1a	0.99	0.997	−3.348	25.581

of the GLRaV-3 positive samples based on melting curve analysis.

Supplementary Table 1 related to this article can be found, in the online version, at <http://dx.doi.org/10.1016/j.jviromet.2014.09.022>.

#### 3.4. Primer efficiency

The PCR efficiencies for all primer sets were calculated from the standard curve slopes using the Rotor-Gene Q software. All PCRs performed, using the pooled cDNA dilution series, showed high efficiencies (0.99–1.02) and high linearity with  $r^2 > 0.991$  (Table 2). The PCR efficiencies of GLRaV-3 single variant infections were also compared (Table 3). For primer set ORF1a, efficiencies were  $> 0.97$  and for the CP and 3'UTR primer sets the efficiencies were  $> 0.91$ . The coefficient of variation of the standard curve slopes between variant groups was 1.20% for the ORF1a assay, 2.7% for the CP assay and 3.27% for the 3'UTR assay (Table 3).

#### 3.5. Intra- and inter-assay variation

To confirm reproducibility of the qPCR assays the intra- and inter-assay variation were calculated. The third dilution of the pooled cDNA dilution series was included in all runs to detect the inter-assay variation and normalise all reactions accordingly. Reproducibility was high with an intra-assay coefficient of variation  $< 0.52\%$  and an inter-assay coefficient of variation  $< 2.09\%$  (Table 4). The  $C_q$  variation at the lower limit was also evaluated. The average standard deviation of  $C_q$  values across all primers for the second to fifth dilution ranged from 0.04 to 0.12, with a 0.25 average standard deviation for the sixth dilution.

#### 3.6. DNA contamination

To evaluate the extent of DNA contamination in all samples, an intron-spanning primer set for the actin gene was used. The actin primer set produced an amplicon of 82 bp if only RNA was present and an amplicon of 165 bp if DNA was also present. DNase-treated total RNA of all samples used in this study was subjected to cDNA synthesis without adding the reverse transcriptase. PCRs with the actin primers were performed using a 1:24 dilution as for the qPCR experiments. Reaction controls included “no-template” controls, “no-DNase-treated RNA” controls and “reverse transcriptase positive cDNA” controls. Amplification with a  $C_q$  value  $> 30$  was observed in 36% of samples. The 165 bp amplicon were present in all of these samples as well as in the “no-DNase-treated RNA” controls. Only the 82 bp amplicon was observed in the “reverse transcriptase positive cDNA” controls.

#### 3.7. Relative limit of detection

In order to be able to compare the primer sets targeting the GLRaV-3 genome, the relative limit of detection (rLOD) of each

**Table 3**  
Comparison of PCR efficiencies and standard curve slope of GLRaV-3 single variant infection assays.

	ORF1a		CP		3'UTR	
	Efficiency	Slope	Efficiency	Slope	Efficiency	Slope
Group I	1.00	−3.32	0.96	−3.42	0.91	−3.51
Group II	1.00	−3.33	0.98	−3.38	0.93	−3.57
Group III	0.97	−3.40	1.00	−3.32	0.95	−3.44
Group VI	1.00	−3.32	0.94	−3.47	0.91	−3.57
GH24	1.01	−3.30	0.91	−3.56	1.01	−3.30
Mean	1.00	−3.33	0.96	−3.43	0.94	−3.48
Standard deviation	0.02	0.04	0.03	0.09	0.04	0.11
Coefficient of variation (%)	1.52	1.20	3.65	2.70	4.40	3.27

**Table 4**  
Intra- and inter-assay variation calculated from the same cDNA dilution included in all experimental Rotor-Gene Q qPCR runs.

Primer set	Intra-assay variation (n = 3)			Inter-assay variation (n = 3)		
	Mean $C_q$	Standard deviation	Coefficient of variation	Mean $C_q$	Standard deviation	Coefficient of variation
ORF1a	19.37	0.10	0.52	19.65	0.24	1.22
CP	18.62	0.01	0.05	18.96	0.40	2.09
3'UTR	19.91	0.04	0.21	19.95	0.05	0.23

primer-specific assay was determined. For all primer sets, real-time PCR and end-point PCR assays were performed. The primer sets targeting ORF1a and the CP were able to detect GLRaV-3 in all real-time PCRs up to the seventh dilution (ORF1a  $C_q = 29.5$  and CP  $C_q = 28.5$ ) and up to the fifth and third dilution in end-point PCR, respectively. The 3'UTR primer set could detect GLRaV-3 in the sixth dilution ( $C_q = 26.4$ ) in real-time PCR and up to the third dilution in end-point PCR. Amplicon specificity was confirmed in all dilutions with melting curve analysis (real-time PCR) and gel electrophoresis (real-time PCR and end-point PCR).

### 3.8. Reference gene stability

In order to analyse the expression stability of reference genes, results from two Excel-based applications, Normfinder and BestKeeper, were compared. The candidate genes were ranked in Normfinder according to their expression stability by calculating a stability value with a standard error for each candidate gene. GAPDH was ranked the most stable reference gene followed by

**Table 5**  
Normfinder stability test.

Reference gene	Stability value	Standard error
actin	0.012	0.002
GAPDH	0.008	0.002
UBC	0.023	0.003
$\alpha$ -Tubulin	0.008	0.002
EF1 $\alpha$	0.020	0.003

$\alpha$ -tubulin, actin, EF1 $\alpha$  and UBC (Table 5). Descriptive statistics were calculated and pair-wise correlation analyses were performed with BestKeeper. The  $C_q$  standard deviation of candidate genes was <0.523 with EF1 $\alpha$  exhibiting the greatest variation (Table 6). Pair-wise correlation analysis between candidate genes showed that UBC had the weakest correlation with the other candidate genes (<0.444) (Table 6). A BestKeeper index was calculated using the geometric mean of the candidate genes'  $C_q$  values. Pairwise correlation analysis between each candidate gene and the index was performed to describe each candidate gene's contribution to the index

**Table 6**  
BestKeeper descriptive statistics of candidate reference genes, pairwise correlation between reference genes and pairwise comparison between each reference gene and the calculated Bestkeeper index.

	Candidate reference genes				
	actin	GAPDH	UBC	$\alpha$ -tubulin	EF1 $\alpha$
Number of samples	30	30	30	30	30
Geometric mean ( $C_q$ )	16.991	19.904	20.987	19.249	24.475
Arithmetic mean ( $C_q$ )	16.996	19.910	20.992	19.255	24.484
Minimum ( $C_q$ )	16.340	19.080	20.140	18.450	23.340
Maximum ( $C_q$ )	18.320	21.340	22.110	20.710	25.910
Standard deviation ( $\pm C_q$ )	0.313	0.422	0.320	0.414	0.523
Coefficient of variation (% $C_q$ )	1.844	2.121	1.525	2.152	2.136
Pearson correlation coefficient (r) analysis					
vs.					
GAPDH	0.829	–	–	–	–
p-value	0.001	–	–	–	–
UBC	0.444	0.440	–	–	–
p-value	0.014	0.015	–	–	–
$\alpha$ -Tubulin	0.824	0.897	0.424	–	–
p-value	0.001	0.001	0.019	–	–
EF1 $\alpha$	0.580	0.736	0.149	0.697	–
p-value	0.001	0.000	0.430	0.001	–
BestKeeper index vs.					
Correlation coefficient (r)	0.892	0.951	0.562	0.936	0.784
p-value	0.001	0.001	0.001	0.001	0.001

**Table 7**  
Bonferroni-type adjusted *p*-values for *t*-tests to determine statistical significant differences between the plant segments, genomic regions, and variant groups, respectively. Significant *p*-values indicated in bold.

A. Two-sided <i>t</i> -tests for plant segments and genomic regions, for each of the two variant groups					
Effect	Plant segment/GLRaV-3 genomic region	Plant segment/GLRaV-3 genomic region	Variant group II Adj <i>p</i> -value	Variant group VI Adj <i>p</i> -value	
Plant segment	1	2	1.0000	1.0000	
Plant segment	1	3	1.0000	0.3471	
Plant segment	1	4	<b>0.0383</b>	<b>0.0384</b>	
Plant segment	1	5	0.0776	<b>0.0020</b>	
Plant segment	2	3	1.0000	0.5169	
Plant segment	2	4	<b>0.0212</b>	0.1648	
Plant segment	2	5	<b>0.0431</b>	0.0654	
Plant segment	3	4	0.6506	0.1719	
Plant segment	3	5	0.6436	0.2036	
Plant segment	4	5	1.0000	1.0000	
Genomic region <sup>a</sup>	3'UTR	CP	0.0991	<b>0.0012</b>	
Genomic region <sup>a</sup>	3'UTR	ORF1a	<b>0.0275</b>	<b>0.0022</b>	
Genomic region <sup>a</sup>	CP	ORF1a	1.0000	1.0000	
B. Two-sided <i>t</i> -tests for variant status and plant segments, for each of the three genomic regions					
Effect	Variant status/Plant segment	Variant status/Plant segment	ORF1a Adj <i>p</i> -value	CP Adj <i>p</i> -value	3'UTR Adj <i>p</i> -value
Variant status <sup>b</sup>	Group II	Group VI	<b>0.0206</b>	<b>0.0428</b>	<b>0.0047</b>
Plant segment	1	2	1.0000	1.0000	1.0000
Plant segment	1	3	0.2378	0.4044	1.0000
Plant segment	1	4	<b>0.0098</b>	<b>0.0082</b>	0.3076
Plant segment	1	5	<b>0.0039</b>	<b>0.0026</b>	<b>0.0327</b>
Plant segment	2	3	1.0000	1.0000	1.0000
Plant segment	2	4	0.1851	0.1054	0.1294
Plant segment	2	5	0.0777	<b>0.0341</b>	<b>0.0128</b>
Plant segment	3	4	1.0000	0.9678	1.0000
Plant segment	3	5	0.8621	0.3643	0.1527
Plant segment	4	5	1.0000	1.0000	1.0000

<sup>a</sup> Using error estimate from linear mixed effect model for variant group status (including the within plant effect).

<sup>b</sup> Using error estimate from linear mixed effect model for genomic region (including the within plant effect).

(Table 6). The analysis showed a strong correlation for GAPDH,  $\alpha$ -tubulin and actin ( $0.892 < r < 0.951$ ) and lower correlations for EF1 $\alpha$  (0.784) and UBC (0.562).

### 3.9. GLRaV-3 quantitation

The GLRaV-3 VCR was measured with three different assays in 5 different segments of actively growing plants. Normalisation of the virus concentration was performed using the three most stable reference genes, actin, GAPDH and  $\alpha$ -tubulin. For both GLRaV-3 variant groups (II and VI) significantly lower VCRs were observed in plant segment 1 compared to segment 5 for the ORF1a, CP and 3'UTR assays (Table 7A and B). Additionally, the VCR for both variant groups was significantly lower when using the 3'UTR assay compared to the ORF1a assay (Table 7A). No significant difference was observed between the VCRs of ORF1a and the CP (Table 7A). The variant groups differed significantly from each other for the 3'UTR, CP and ORF1a assays, with variant group II having higher VCRs compared to variant group VI (Table 7B, Fig. 1).

## 4. Discussion

The aims of this study were to develop a sensitive and accurate assay for the relative quantitation of GLRaV-3 and to identify the most suitable genomic region to target for GLRaV-3 quantitation. Plants infected with the most prevalent variants groups of GLRaV-3 in South Africa, II and VI (Jooste et al., 2012), were selected in order to see if a difference in virus concentration could be detected. Five different segments were collected from each plant and three primer sets, targeting different GLRaV-3

genomic regions, were used to measure relative virus concentration.

The specificity of all primer sets was confirmed by gel electrophoresis, Sanger sequencing, melting curve analysis and by calculating the  $C_q$  value of primer-dimers. Primer-dimers were detectable in no-template controls of the CP and actin primer sets and in the plant negative controls of the ORF1a and CP primer set. However, primer-dimers were easily distinguishable on melt profiles and all  $C_q$  values > 30 proved to be the result of primer dimers. To test for the extent of DNA contamination in samples a primer set targeting an intron-spanning region of the actin gene was used to amplify DNase-treated RNA. Amplification with a  $C_q$  value > 30 was observed in 36% of the samples and determined to be due to DNA contamination. Therefore, any amplification in samples after 30 cycles would not have been considered accurate  $C_q$  values. However, no cDNA samples produced  $C_q$  values > 22 and as a result was considered as a true representation of the concentration of reference genes.

The PCR efficiencies and linearity calculated from all assays' standard curves were high and no evidence of inhibition was seen from the  $C_q$  values of the dilution series. All standard curves were constructed with pooled cDNA samples to ensure that the standard curve is a true representation of the virus infection being quantitated. The frequent occurrence of mixed GLRaV-3 variant infections combined with the high mutation rate of RNA viruses means that a virus infection is not represented by a single genome but rather by a related pool of sequences. Therefore, the efficiency of all GLRaV-3 specific primers had to be evaluated for different variant group infections separately. The primer set targeting ORF1a had the highest and most equal efficiencies for the five variants evaluated. However, all three GLRaV-3 specific primer sets had an efficiency > 0.91 for the single variant infections analysed. Since the

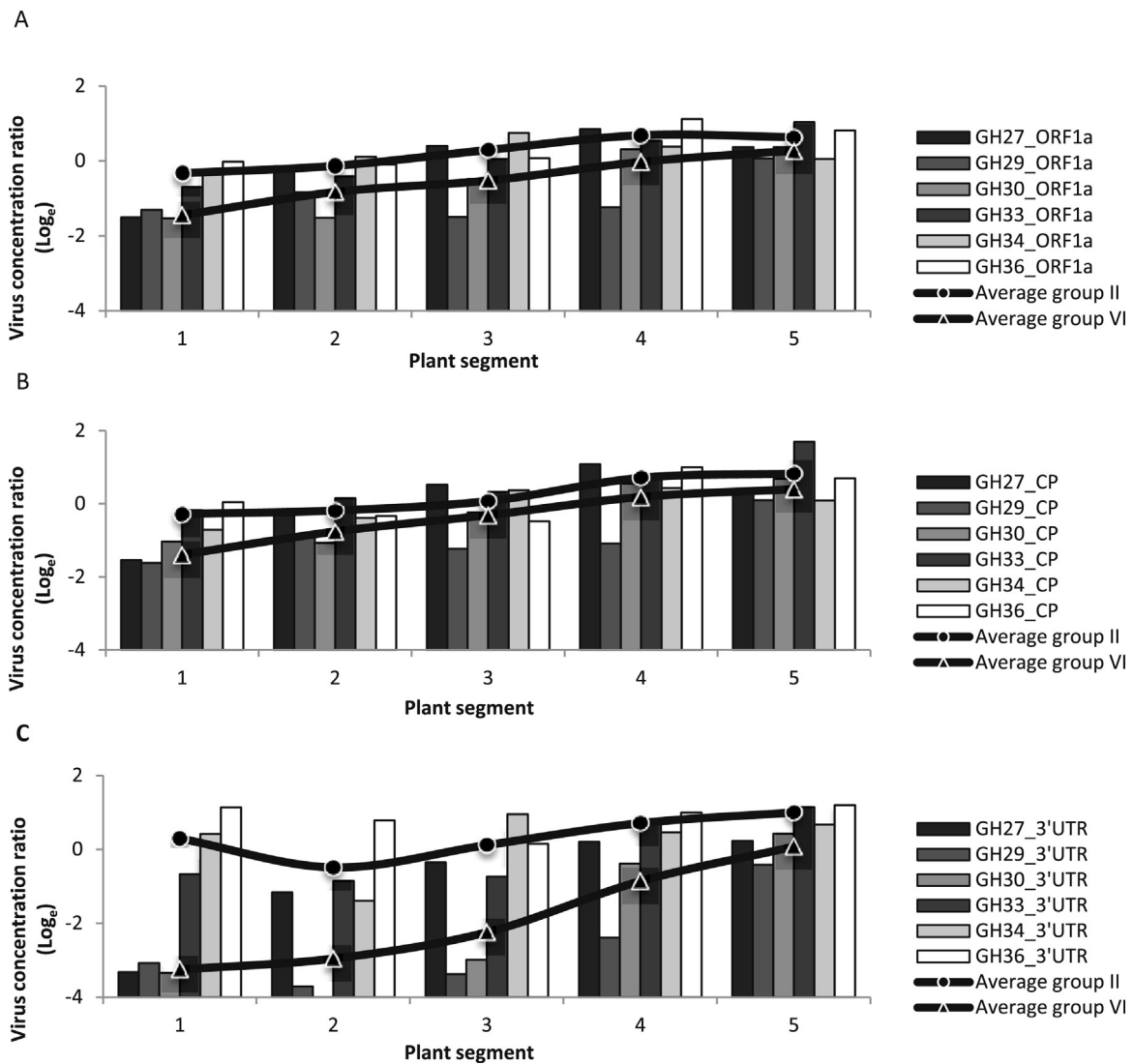


Fig. 1. Natural logarithm of the virus concentration ratio (VCR) calculated for each plant segment measured with the three GLRaV-3 assays (A:ORF1a, B:CP, C:3'UTR).

standard curve slopes' coefficient of variation was <3.27% between variant groups for the three assays, it can be concluded that none of the three primer sets display any bias towards a specific variant group should mixed infections occur.

The intra- and inter-assay variation revealed no significant differences between runs and showed high reproducibility for all three GLRaV-3 assays. The low inter-assay variation also confirmed the integrity of the cDNA dilutions throughout the study. By evaluating the  $C_q$  variation at each serial dilution the average standard deviation for the sixth dilution was higher compared to the second to fifth dilutions for all primer sets. This may suggest that even though detection will be possible for further dilutions, accurate quantitation may not be possible beyond the sixth or seventh dilution. To assess the sensitivity the rLOD of the GLRaV-3 assays was determined using the same dilution series in all assays. The ORF1a and CP assays were equally sensitive with ORF1a being the most sensitive end-point PCR assay.

Accurate normalisation of the gene of interest is a prerequisite for reliable relative quantitation results. Tissue types, integrity of RNA, loading error and enzyme or primer performance are some of the parameters that can influence accurate quantitation. Therefore, the use of only one reference gene for normalisation can lead to the over or under estimation of relative transcript abundance.

In this study the expression stability of five reference genes in GLRaV-3 infected phloem material was analysed. According to the BestKeeper results, the expression stability of all five genes can be considered consistent since the  $C_q$  standard deviations of all genes were smaller than 1.0. However, pairwise correlation analysis between candidate genes showed the smallest correlation for EF1 $\alpha$  and UBC. Normfinder similarly ranked EF1 $\alpha$  and UBC as the least stable reference genes compared to GAPDH,  $\alpha$ -tubulin and actin. In this study, GAPDH,  $\alpha$ -tubulin and actin were used for normalisation of GLRaV-3 concentration. It was concluded that a reference gene index calculated from three genes represents a balance between realistic laboratory practices and accurate quantitation.

In this study, GLRaV-3 was quantitated using a relative quantitation model with efficiency correction. An efficiency corrected mathematical model is strongly recommended since small efficiency differences between target and reference gene can result in a false expression ratio (Pfaffl, 2004). Due to the high diversity of the GLRaV-3 genome and the influence of the virus on the plant a relative quantitation model with reference gene index normalisation proved the most suitable quantitation technique for GLRaV-3.

A significant difference in virus concentration was observed in all samples infected with the two different GLRaV-3 variant groups.

Since the difference was observed with all three assays, it may suggest that the replication tempo of genetic variant group II is faster than group VI. It has been suggested that the 3' genes of GLRaV-3 is expressed through a set of 3' co-terminal sgRNAs (Jarugula et al., 2010; Maree et al., 2010). This increase in templates for the viral genes at the 3' end of the GLRaV-3 genome is generally considered to make better targets for diagnostic RT-PCR assays (Osman et al., 2008, 2007; Bester et al., 2012b). Many studies also state that the RNA-dependent RNA polymerase (RdRp) domain is preferred for the calculation of the number of viral genomes to avoid the over-estimation that may result from genes that are shared between genomic and subgenomic RNAs (Ruiz-Ruiz et al., 2007; Pacifico et al., 2011; Tsai et al., 2012; Velasco et al., 2013). In this study primers were designed that targeted three different regions of the GLRaV-3 genome, believed to be represented by different levels of sgRNAs (Jarugula et al., 2010; Maree et al., 2010). Significant lower 3'UTR VCRs compared to the CP assay were observed for both variant groups II and VI, with no significant difference between ORF1a and the CP. This may suggest a possible sgRNA influence, but since this finding is contrary to what was expected further investigation is needed. Different patterns of sgRNA levels may be detected at different time points throughout the season and therefore sampling at only one time point may have limited this study. The use of random primers for cDNA synthesis might have resulted in uneven priming across the genome. However, to ensure that the gene expression results can be compared directly between the applied assays for gene of interest normalisation, random primers were used. Quantitation of different viral genes in temporal and spatial experiments can contribute to elucidating the virus replication strategy and provide possible links between variant status and symptom severity.

In all six plants, measured with the three primer sets, the virus concentration was significantly higher in segment 5 (new growth) compared to segment 1 (oldest growth). This implies that GLRaV-3 moves through the plant and actively replicates in new growing material.

## 5. Conclusion

In this study three GLRaV-3 relative quantitation assays using SYBR green chemistry were developed. The assays had high reproducibility and specificity and were more sensitive than conventional end-point RT-PCR. These assays are the first Minimum Information for publication of Quantitative real-time PCR Experiments (MIQE) guidelines compliant (Bustin et al., 2009) relative quantitation system for GLRaV-3, using the PCR efficiency correction model. These guidelines were developed to ensure the integrity of qPCR assays, facilitate reproducibility and increase experimental transparency. All three assays are able to detect all known GLRaV-3 variant groups present in South Africa, including isolate GH24, with equal efficiency. GAPDH,  $\alpha$ -tubulin and actin were identified as stably expressed reference genes in GLRaV-3 infected phloem material, suitable for gene of interest normalisation. GLRaV-3 was quantitated using three GLRaV-3 genomic regions and even though significant differences between genes located in the 5' region of the genome vs. the 3'UTR were observed, no direct link between GLRaV-3 concentration and sgRNA expression could be established. The GLRaV-3 VCR between variant groups II and VI was also evaluated and a significantly lower concentration for variant group VI was observed. Significantly greater virus accumulation was also detected in the actively growing plant segments.

These GLRaV-3 RT-qPCR assays can be used as tools in plant-virus interaction studies to determine the effects of GLRaV-3 variant groups, geographical distribution, host cultivar or the application of different treatments on virus concentration. The VCR can

also be used to monitor disease spread in individual vines or vineyards to resolve GLD aetiology.

## Acknowledgements

The financial assistance of the National Research Foundation (NRF) towards this research is hereby acknowledged. Opinions expressed and conclusions arrived at, are those of the authors and are not necessarily to be attributed to the NRF.

## References

- Altman, D.G., 1990. Practical statistics for medical research. In: Chapman & Hall/CRC Texts in Statistical Science. Taylor & Francis, London.
- Andersen, C.L., Jensen, J.L., Ørntoft, T.F., 2004. Normalization of real-time quantitative reverse transcription-PCR data: a model-based variance estimation approach to identify genes suited for normalization, applied to bladder and colon cancer data sets. *Cancer Res.* 64, 5245–5250.
- Bester, R., Jooste, A.E.C., Maree, H.J., Burger, J.T., 2012a. Real-time RT-PCR high-resolution melting curve analysis and multiplex RT-PCR to detect and differentiate grapevine leafroll-associated virus 3 variant groups I, II, III and VI. *Virol. J.* 9, <http://dx.doi.org/10.1186/1743-422X-9-219>.
- Bester, R., Maree, H.J., Burger, J.T., 2012b. Complete nucleotide sequence of a new strain of grapevine leafroll-associated virus 3 in South Africa. *Arch. Virol.* 157, 1815–1819, <http://dx.doi.org/10.1007/s00705-012-1333-8>.
- Boyd, L.A., Ridout, C., O'Sullivan, D.M., Leach, J.E., Leung, H., 2013. Plant-pathogen interactions: disease resistance in modern agriculture. *Trends Genet.* 29, 233–240, <http://dx.doi.org/10.1016/j.tig.2012.10.011>.
- Bustin, S.A., 2000. Absolute quantification of mRNA using real-time reverse transcription polymerase chain reaction assays. *J. Mol. Endocrinol.* 25, 169–193.
- Bustin, S.A., Benes, V., Garson, J.A., Hellems, J., Huggett, J., Kubista, M., Mueller, R., Nolan, T., Pfaffl, M.W., Shipley, G.L., Vandesompele, J., Wittwer, C.T., 2009. The MIQE guidelines: minimum information for publication of quantitative real-time PCR experiments. *Clin. Chem.* 55, 611–622, <http://dx.doi.org/10.1373/clinchem.2008.112797>.
- Carra, A., Gambino, G., Schubert, A., 2007. A cetyltrimethylammonium bromide-based method to extract low-molecular-weight RNA from polysaccharide-rich plant tissues. *Anal. Biochem.* 360, 318–320, <http://dx.doi.org/10.1016/j.ab.2006.09.022>.
- Chooi, K.M., Cohen, D., Pearson, M.N., 2013a. Molecular characterisation of two divergent variants of grapevine leafroll-associated virus 3 in New Zealand. *Arch. Virol.* 158, 1597–1602, <http://dx.doi.org/10.1007/s00705-013-1631-9>.
- Chooi, K.M., Cohen, D., Pearson, M.N., 2013b. Generic and sequence-variant specific molecular assays for the detection of the highly variable Grapevine leafroll-associated virus 3. *J. Virol. Methods* 189, 20–29, <http://dx.doi.org/10.1016/j.jviromet.2012.12.018>.
- Cohen, D., Chooi, K.M., Bell, V.A., Blouin, A.G., Pearson, M.N., MacDiarmid, R.M., 2012. Detection of new strains of GLRaV-3 in New Zealand using ELISA and RT-PCR. In: Proceedings of the 17th Congress of the International Council for the Study of Virus and Virus-like Diseases of the Grapevine (ICVG), October 7–14, 2012, Davis, CA, USA, pp. 118–119.
- Engel, E.A., Girardi, C., Escobar, P.F., Arredondo, V., Domínguez, C., Pérez-Acle, T., Valenzuela, P.D.T., 2008. Genome analysis and detection of a Chilean isolate of Grapevine leafroll associated virus-3. *Virus Genes* 37, 110–118, <http://dx.doi.org/10.1007/s11262-008-0241-1>.
- Eun, A.J.-C., Seah, M.-L., Wong, S.-M., 2000. Simultaneous quantitation of two orchid viruses by the TaqMan® real-time RT-PCR. *J. Virol. Methods* 87, 151–160, [http://dx.doi.org/10.1016/S0166-0934\(00\)00161-0](http://dx.doi.org/10.1016/S0166-0934(00)00161-0).
- Fei, F., Lyu, M.-D., Li, J., Fan, Z.-F., Cheng, Y.-Q., 2013. Complete nucleotide sequence of a Chinese isolate of Grapevine leafroll-associated virus 3 reveals a 5' UTR of 802 nucleotides. *Virus Genes* 46, 182–185, <http://dx.doi.org/10.1007/s11262-012-0823-9>.
- Goszczyński, D.E., 2013. Brief report of a new highly divergent variant of grapevine leafroll-associated virus 3 (GLRaV-3). *J. Phytopathol.* 161, 874–879, <http://dx.doi.org/10.1111/jph.12139>.
- Gouveia, P., Santos, M.T., Eiras-Dias, J.E., Nolasco, G., 2011. Five phylogenetic groups identified in the coat protein gene of grapevine leafroll-associated virus 3 obtained from Portuguese grapevine varieties. *Arch. Virol.* 156, 413–420, <http://dx.doi.org/10.1007/s00705-010-0878-7>.
- Jarugula, S., Gowda, S., Dawson, W.O., Naidu, R.A., 2010. 3'-coterminal subgenomic RNAs and putative cis-acting elements of Grapevine leafroll-associated virus 3 reveals unique features of gene expression strategy in the genus Ampelovirus. *Virol. J.* 7, <http://dx.doi.org/10.1186/1743-422X-7-180>.
- Jooste, A.E.C., Bester, R., Maree, H.J., De Koker, W., Burger, J.T., 2012. A survey of red and white cultivars to test an improved detection technique for grapevine leafroll associated virus 3 (GLRaV-3) variants identified in South African vineyards. In: Proceedings of the 17th Congress of the International Council for the Study of Virus and Virus-like Diseases of the Grapevine (ICVG), October 7–14, 2012, Davis, CA, USA, pp. 122–123.
- Jooste, A.E.C., Maree, H.J., Bellstedt, D.U., Goszczyński, D.E., Pietersen, G., Burger, J.T., 2010. Three genetic grapevine leafroll-associated virus 3 variants identified



- from South African vineyards show high variability in their 5'UTR. Arch. Virol. 15, 5, <http://dx.doi.org/10.1007/s00705-010-0793-y>.
- López-Fabuel, I., Wetzels, T., Bertolini, E., Bassler, A., Vidal, E., Torres, L.B., Yuste, A., Olmos, A., 2013. Real-time multiplex RT-PCR for the simultaneous detection of the five main grapevine viruses. J. Virol. Methods 188, 21–24, <http://dx.doi.org/10.1016/j.jviromet.2012.11.034>.
- Maree, H., Freeborough, M., Burger, J., 2008. Complete nucleotide sequence of a South African isolate of grapevine leafroll-associated virus 3 reveals a 5'UTR of 737 nucleotides. Arch. Virol. 153, 755–757.
- Maree, H.J., Almeida, R.P.P., Bester, R., Chooi, K.M., Cohen, D., Dolja, V.V., Fuchs, M.F., Golino, D.A., Jooste, A.E.C., Martelli, G.P., Naidu, R.A., Rowhani, A., Saldarelli, P., Burger, J.T., 2013. Grapevine leafroll-associated virus 3. Front. Microbiol. 4, <http://dx.doi.org/10.3389/fmicb.2013.00082>.
- Maree, H.J., Gardner, H.F.J., Freeborough, M.-J., Burger, J.T., 2010. Mapping of the 5' terminal nucleotides of Grapevine leafroll-associated virus 3 sgRNAs. Virus Res. 151, 252–255, <http://dx.doi.org/10.1016/j.virusres.2010.05.011>.
- Margarita, P., Turina, M., Palmano, S., 2009. Detection of Flavescence dorée and Bois noir phytoplasmas. Grapevine leafroll associated virus-1 and -3 and Grapevine virus A from the same crude extract by reverse transcription real-time Taqman assays. Plant Pathol. 58, 838–845, <http://dx.doi.org/10.1111/j.1365-3059.2009.02119.x>.
- Martelli, G.P., Abou Ghanem-Sabanadzovic, N., Agranovsky, A.A., Al Rwahnih, M., Dolja, V.V., Dovas, C.I., Fuchs, M., Gugerli, P., Hu, J.S., Jelkmann, W., 2012. Taxonomic revision of the family Closteroviridae with special reference to the grapevine leafroll-associated members of the genus Ampelovirus and the putative species unassigned to the family. J. Plant Pathol. 94, 7–19.
- Martelli, G.P., Boudon-Padieu, E., 2006. Directory of Infectious Diseases of Grapevines and Viruses and Virus-like Diseases of the Grapevine: Bibliographic Report 1998–2004. Options méditerranéennes: serie B: Studies and Research. CIHEAM.
- Osman, F., Leutenegger, C., Golino, D., Rowhani, A., 2007. Real-time RT-PCR (TaqMan®) assays for the detection of Grapevine Leafroll associated viruses 1–5 and 9. J. Virol. Methods 141, 22–29.
- Osman, F., Leutenegger, C., Golino, D., Rowhani, A., 2008. Comparison of low-density arrays, RT-PCR and real-time TaqMan® RT-PCR in detection of grapevine viruses. J. Virol. Methods 149, 292–299.
- Osman, F., Rowhani, A., 2006. Application of a spotting sample preparation technique for the detection of pathogens in woody plants by RT-PCR and real-time PCR (TaqMan). J. Virol. Methods 133, 130–136, <http://dx.doi.org/10.1016/j.jviromet.2005.11.005>.
- Pacifico, D., Caciagli, P., Palmano, S., Mannini, F., Marzachi, C., 2011. Quantitation of Grapevine leafroll associated virus-1 and -3, Grapevine virus A Grapevine fanleaf virus and Grapevine fleck virus in field-collected *Vitis vinifera* L. Nebbiolo by real-time reverse transcription-PCR. J. Virol. Methods 172, <http://dx.doi.org/10.1016/j.jviromet.2010.12.002>.
- Pfaffl, M., Tichopad, A., Prgomet, C., Neuvians, T., 2004. Determination of stable housekeeping genes, differentially regulated target genes and sample integrity: BestKeeper—Excel-based tool using pair-wise correlations. Biotechnol. Lett. 26, 509–515, <http://dx.doi.org/10.1023/B:BILE.0000019559.84305.47>.
- Pfaffl, M.W., 2001. A new mathematical model for relative quantification in real-time RT-PCR. Nucleic Acids Res. 29, e45, <http://dx.doi.org/10.1093/nar/29.9.e45>.
- Pfaffl, M.W., 2004. Quantification strategies in real-time PCR. A-Z Quant. PCR 1, 89–113.
- Prosser, S.W., Goszczynski, D.E., Meng, B., 2007. Molecular analysis of double-stranded RNAs reveals complex infection of grapevines with multiple viruses. Virus Res. 124, 151–159, <http://dx.doi.org/10.1016/j.virusres.2006.10.014>.
- Rasmussen, R., 2001. Quantification on the LightCycler instrument. In: Meuer, S., Wittwer, C., Nakagawara, K. (Eds.), Rapid Cycle Real-Time PCR: Methods and Applications. Springer-Verlag Press, Heidelberg, pp. 21–34.
- Reid, K., Olsson, N., Schlosser, J., Peng, F., Lund, S., 2006. An optimized grapevine RNA isolation procedure and statistical determination of reference genes for real-time RT-PCR during berry development. BMC Plant Biol. 6, 1–11, <http://dx.doi.org/10.1186/1471-2229-6-27>.
- Roberts, C.A., Dietzgen, R.G., Heelan, L.A., Maclean, D.J., 2000. Real-time RT-PCR fluorescent detection of tomatto spotted wilt virus. J. Virol. Methods 88, 1–8.
- Ruiz-Ruiz, S., Moreno, P., Guerri, J., Ambrós, S., 2007. A real-time RT-PCR assay for detection and absolute quantitation of Citrus tristeza virus in different plant tissues. J. Virol. Methods 145, 96–105, <http://dx.doi.org/10.1016/j.jviromet.2007.05.011>.
- Seah, Y., Sharma, A.M., Zhang, S., Almeida, R.P., Duffy, S., 2012. A divergent variant of Grapevine leafroll-associated virus 3 is present in California. Virol. J. 9, <http://dx.doi.org/10.1186/1743-422X-9-235>.
- Sharma, A.M., Wang, J., Duffy, S., Zhang, S., Wong, M.K., Rashed, A., Cooper, M.L., Daane, K.M., Almeida, R.P.P., 2011. Occurrence of grapevine leafroll-associated virus complex in Napa Valley. PLoS ONE 6, <http://dx.doi.org/10.1371/journal.pone.0026227>.
- Snijders, T.A.B., Bosker, R.J., 1999. Multilevel Analysis: An Introduction to Basic and Advanced Multilevel Modeling. Sage Publications, London.
- Terrier, N., Glissant, D., Grimplet, J., Barriau, F., Abbal, P., Couture, C., Ageorges, A., Atanassova, R., Léon, C., Renaudin, J.-P., Dédaldéchamp, F., Romieu, C., Delrot, S., Hamdi, S., 2005. Isogene specific oligo arrays reveal multifaceted changes in gene expression during grape berry (*Vitis vinifera* L.) development. Planta 222, 832–847, <http://dx.doi.org/10.1007/s00425-005-0017-y>.
- Tsai, C.W., Daugherty, M.P., Almeida, R.P.P., 2012. Seasonal dynamics and virus translocation of Grapevine leafroll-associated virus 3 in grapevine cultivars: seasonal dynamics of GLRaV-3 in grapevines. Plant Pathol. 61, 977–985, <http://dx.doi.org/10.1111/j.1365-3059.2011.02571.x>.
- Vandesompele, J., De Preter, K., Pattyn, F., Poppe, B., Van Roy, N., De Paepe, A., Speleman, F., 2002. Accurate normalization of real-time quantitative RT-PCR data by geometric averaging of multiple internal control genes. Genome Biol. 3 (7), <http://dx.doi.org/10.1186/gb-2002-3-7-research0034>, research0034-research0034.11.
- Velasco, L., Bota, J., Montero, R., Cretazzo, E., 2013. Differences of three ampeloviruses' multiplication in plant may explain their incidences in vineyards. Plant Dis. 98, 395–400, <http://dx.doi.org/10.1094/PDIS-04-13-0433-RE>.
- Wang, J., Sharma, A.M., Duffy, S., Almeida, R.P., 2011. Genetic diversity in the 3' terminal 4.7-kb region of Grapevine leafroll-associated virus 3. Phytopathology 101, 445–450.